Quantifying the role of orographic processes in producing extreme precipitation: a case study of an atmospheric river associated with storm Bronagh

JGR Atmospheres

RESEARCH ARTICLE
10.1029/2023JD040557

Quantifying the Role of Orographic Processes in Producing Extreme Precipitation: A Case Study of an Atmospheric River Associated With Storm Bronagh

S. Cuckow[1], H. F. Dacre[1], O. Martínez-Alvarado[1,2], and S. A. Smith[3]

[1]Department of Meteorology, University of Reading, Reading, UK, [2]National Centre for Atmospheric Science, University of Reading, Reading, UK, [3]Met Office, Exeter, UK

Key Points:

- The largest contribution to observed rainfall totals (63%) was associated with frontal ascent and convection in storm Bronagh
- Interaction of storm Bronagh with orography enhanced rainfall totals by a further 50%
- Orographic rainfall enhancement in storm Bronagh is dominated by the seeder-feeder process

Correspondence to:

H. F. Dacre,
h.f.dacre@reading.ac.uk

Citation:

Cuckow, S., Dacre, H. F., Martínez-Alvarado, O., & Smith, S. A. (2024). Quantifying the role of orographic processes in producing extreme precipitation: A case study of an atmospheric river associated with storm Bronagh. *Journal of Geophysical Research: Atmospheres*, *129*, e2023JD040557. https://doi.org/10.1029/2023JD040557

Received 5 DEC 2023
Accepted 22 AUG 2024

Abstract This study explores the mechanisms contributing to heavy precipitation associated with landfalling atmospheric rivers (ARs) and orography, focusing on a high-profile case study of an extratropical cyclone, storm Bronagh, which caused flooding and travel disruption in the UK. While prior research has established the connection between ARs, orography, and precipitation, the specific mechanisms leading to intense rainfall remain unclear. A novel methodology is introduced that quantifies the relative contribution to the total precipitation from cyclone-induced processes and orographic processes using modifications to the Met Office Unified Model orography and microphysics parameterization scheme. Results show that the majority (63%) of storm Bronagh 's rainfall over land is attributed to cyclone-related processes (frontal ascent and embedded convection). However, interaction of the AR associated with storm Bronagh and orography focuses more of the rain over the hills, enhancing precipitation in this region by a further 50%. Further analysis reveals that the seeder-feeder mechanism plays a predominant role in orographically enhanced rainfall. Accretion and riming processes occur as rain from the cyclone induced (seeder) cloud falls through the orographically induced (feeder) cloud enhancing precipitation rates. The feeder cloud formation is related to forced ascent of air within the AR over the orography. In conclusion, this study sheds light on the intricate interplay between ARs, orography, and cyclone precipitation during the landfall of extratropical cyclones. By separating the mechanisms behind heavy rainfall in the context of storm Bronagh, we quantify for the first time the effect of the seeder-feeder effect at different heights over orography.

Plain Language Summary This study investigates why we experience heavy rainfall during storms in the UK. We focus on storm Bronagh which reached the national news because of the flooding and travel disruption it caused. While there is an established statistical link between atmospheric rivers, mountains, and rain, the details of how atmospheric rivers interact with mountains leading to intense rainfall were not well-understood. In this research, a new approach which made adjustments to a weather model is used to determine these complex interactions. The results showed that most of the heavy rain during storm Bronagh came from the storm itself, but that it was enhanced via interaction with the mountains. The moisture in an atmospheric river turns into cloud droplets as it is forced to rise over the mountains. A specific process, allowing small raindrops to grow rapidly as they fall through orographic cloud, caused the localized rainfall enhancement. Understanding these processes helps us predict and prepare for extreme weather events better, enhancing our ability to respond to their impacts effectively.

1. Introduction

Both extratropical cyclones and atmospheric rivers have been linked to heavy precipitation. Extratropical cyclones contribute to over 50% of precipitation in the northern hemisphere (Hawcroft et al., 2012) and to a high percentage of precipitation extremes globally (Pfahl & Wernli, 2012). Warm conveyor belts specifically are relevant to extreme precipitation in many parts of the extratropics (Pfahl et al., 2014). It has also been found that landfalling atmospheric rivers that coincide with orography can also produce a large amount of precipitation (Gimeno-Sotelo & Gimeno, 2023), particularly along exposed mountain ranges located along west coasts. This has been shown in many studies that focus on the west coast of North America (Lamjiri et al., 2017; Neiman et al., 2011; Ralph et al., 2004, 2006; Rutz et al., 2014), west coasts in Europe (Allan et al., 2016; Champion et al., 2015; Lavers et al., 2011, 2013; Michel et al., 2021; Ramos et al., 2015) and the west coast of New Zealand (Kingston et al., 2016; Kropač et al., 2021; Reid et al., 2021). The heavy precipitation associated with atmospheric

rivers can have a wide variety of impacts. This includes flooding (Lavers et al., 2011), the influence of extreme ablation and snowfall events (Little et al., 2019) and the inducing of surface melting of ice sheets (Oltmanns et al., 2018). Therefore, it is imperative that the mechanisms that lead to the heavy precipitation are understood, particularly as the intensity of atmospheric rivers is expected to increase as the climate warms and there is an increase in atmospheric moisture (Allan et al., 2020).

The ascending and descending flows that occur within an extratropical cyclone are known as conveyor belts (Carlson, 1980). The warm conveyor belt is a moist airflow that ascends from the warm sector ahead of the cold front. It ascends to the upper-troposphere where one branch turns cyclonically to form the upper portion of the comma shaped cloud head and precipitation (Browning, 1971). The cold conveyor belt transports cool, moist air north of the warm front to the west of the low pressure center. The cold conveyor belt sits below the warm conveyor belt and creates the lower portion of the cloud head (Carlson, 1980). Alongside precipitation produced by ascent in the warm and cold conveyor belts, it can also form as a result of embedded convection in the warm conveyor belt and along the fronts (Oertel et al., 2021).

Atmospheric rivers and extratropical cyclones are related via a cyclone-relative low-level airflow called the feeder airstream (Cuckow et al., 2022; Dacre et al., 2015, 2019). The feeder airstream partitions an atmospheric river into two sections, which are referred to as the head and tail of the atmospheric river (Xu et al., 2022). One branch of this airstream feeds moisture to the head of the atmospheric river at the base of the warm conveyor belt where it rises to form precipitation. The other branch runs parallel to the cold front forming the tail of the atmospheric river, and is left behind as the cyclone propagates. The low-level moisture in the tail of the atmospheric river requires an ascent mechanism, such as forced ascent over orography, in order to produce heavy precipitation.

There are many types of orographic processes that can lead to precipitation. The most straightforward example is pure upslope orographic rain, where a cap cloud produced by orographic ascent is able to produce precipitation (Roe, 2005). Orography an also influence precipitation via the triggering of convection if the orography lifts the moist air above its level of free convection (Roe, 2005). Another orographic process leading to precipitation growth is known as the seeder-feeder mechanism. The seeder-feeder mechanism occurs when rainfall from a pre-exisiting precipitating (often frontal) seeder cloud, falls through a cap cloud or orographically enhanced pre-existing low-level cloud, known as the feeder cloud. In this situation the precipitation from the seeder cloud collide and coalesce with cloud droplets in the feeder cloud via a process called accretion. If the freezing level is low enough to coincide with the orographic cloud, then the seeder-feeder mechanism can also occur via a process called riming, in which a falling ice particle collides with nearby water droplets that freeze onto the particle. The upper-level seeder cloud is typically formed via ascent of moist air associated with a frontal system (e.g., in a warm conveyor belt). The lower-level feeder cloud is formed via the orographic ascent of a low-level moist airflow (Hill et al., 1981), such as an atmospheric river, and is often called a cap cloud. Thus, the seeder-feeder mechanism typically occurs when the warm sector of an extratropical cyclone coincides with orography (Bader & Roach, 1977; Browning & Mason, 1980). The seeder-feeder mechanism removes moisture from the atmospheric column over orography, leaving drier air to be advected into the lee-side of the mountain. Therefore, the orographically produced rainfall often lies on the windward side (upstream) of the mountain leaving a rain shadow (area of no rain) on the lee-side (downstream) (AMS, 2023).

The degree of rainfall enhancement within the feeder cloud over a particular hill depends largely on the strength of the low-level winds, the humidity and temperature of the air, and the intensity of precipitation falling from the seeder cloud (Hill et al., 1981; B. Smith et al., 2010; Lean & Browning, 2013). It was found by Hill et al. (1981) that the largest enhancement of rainfall in the case study they investigated, coincided with high winds and relative humidity below 2 km and that 80% of the enhancement occurred in the lowest 1.5 km over the hills. Furthermore, moist air masses below 1 km have been shown to be important in the production of orographic precipitation over the western US and UK (B. Smith et al., 2010; Neiman et al., 2011). This low-level moist flow is consistent with an atmospheric river which typically lies below 3 km. Thus, the observed enhancement of precipitation during the passage of an extratropical cyclone over orography depends on both the moisture flux within the low-level airflow and the precipitation from the upper-level cyclone clouds. In this research, we have designed an experiment to examine and quantify these synoptic, mesoscale and microphysical processes.

Whilst studies such as those by Neiman et al. (2011), Ramos et al. (2015) and Kingston et al. (2016) highlight the link between atmospheric rivers and orographic rainfall (precipitation formed by the influence of orography), they do not discuss the microphysical mechanisms or processes that lead to heavy precipitation. Other studies such as Rössler et al. (2014) show the importance of the seeder-feeder mechanism in the production of precipitation in land-falling atmospheric river case study. Thomas et al. (2023) investigate the effect of atmospheric warming and increased cloud condensation nuclei concentration on precipitation in a case study of an atmospheric river with a mixed phase seeder-feeder mechanism producing precipitation in Cumbria. In their study, a piggyback approach is used to update the changes in the microphysics variables with temperature at each time step whilst leaving the winds and pressure the same. This allows the changes in rainfall attributed to each micro-physical mechanism to be quantified without altering the large scale thermodynamics. However, these studies do not compare how much rainfall is produced by the large-scale ascent and convection in the cyclone warm and cold conveyor belts, to the enhancement of rainfall by microphysical mechanisms and other orographic processes. This study introduces a novel methodology that quantifies the relative contributions of these three different mechanisms that lead to the production of precipitation in the UK. This is achieved using a case study of an impactful case study, storm Bronagh, and its associated atmospheric river. During the passage of this storm and atmospheric river over the UK, flooding occurred in parts of England and Wales (Cuckow et al., 2022) which led to storm Bronagh being reported on in the national news. Through the modification of orography and microphysical processes in the Met Office Unified Model (MetUM), the proportion of the rainfall produced by the cyclone (via the warm and cold conveyor belts, embedded convection along the warm conveyor belt and along the fronts), by the seeder feeder mechanism, and by other possible orographic processes can be quantified. These other orographic processes include orographically enhanced convection and the enhancement of rain by microphysical processes other than accretion and riming.

2. Data and Methods

2.1. The MetUM Model

The model used in this study is the Met Office Unified Model (MetUM) in its UKA4g setup. This setup uses the regional UKV configuration and is implemented using the MetUM version 11.1. The UKV is a limited area model that is nested within the MetUM global model (17 km grid spacing). The hourly lateral boundary conditions for the limited area model are provided by MetUM global model simulation initialized from analysis every 24 hr. The resolution of the UKA4g model is 1.5×1.5 km in the inner regions and 4×4 km around the edges of the domain. The variable resolution at the boundaries of the limited area model allows the lateral boundary conditions to be blended from a low resolution to a high resolution. This means that the lateral boundary conditions are better matched to the limited area model and noise generated by the lateral boundary conditions is reduced (Davies, 2014). The UKA4g domain lies between approximately 46°N to 63°N and 19° W to 13°E (Valiente et al., 2021). It has been shown by S. A. Smith et al. (2015) that on average, orographic precipitation over the UK (including Wales) is accurately reproduced in the MetUM at 1.5 km resolution.

The model has 70 hybrid height vertical levels with a model top at approximately 40 km (Gentile et al., 2021; Lewis et al., 2019). The vertical coordinate system is terrain following near the surface and becomes flat at approximately 30 km above ground level. To investigate the precipitation associated with storm Bronagh, the UKA4g model is run for 72 hr (start time of 00 UTC 19 September 2018), beginning 24 hr before the times used in the analysis to allow for spin-up to the higher resolution.

2.2. Experimental Design

To investigate the amount of rainfall produced via cyclone ascent, orographic processes excluding the seeder-feeder mechanism, and the seeder-feeder mechanism, three experiments are conducted using the UKA4g model during the time that storm Bronagh passes over the UK (00 UTC 20 September 2018 to 00 UTC 22 September 2018). The first experiment (FLAT experiment in table 1) involves flattening the orography in the domain so that no rainfall is produced by the presence of hills. Therefore, only rainfall produced by cyclone-induced processes is present in this experiment. This is shown in Figure 1a and is described by

$$E^{FLAT} = a_c, \tag{1}$$

Table 1
Experiments Performed Through the Modification of Orography, Accretion and Riming Within the UKA4g Model

Experiment	Orography	Accretion and riming schemes	Mechanisms present
FLAT	Flattened	Unmodified	Cyclone processes
NOACC1, NOACC2, NOACC2.5, NOACC3	Unmodified	Off below an altitude of 1, 2, 2.5 and 3 km where the surface height is greater than 200 m	Cyclone processes and other orographic processes (all orographic processes excluding the seeder-feeder mechanism)
CTRL	Unmodified	Unmodified	Cyclone processes, other orographic processes and the seeder-feeder mechanism

where E^{FLAT} denotes the accumulated rainfall produced by this experiment and a_c denotes the accumulated rainfall formed via cyclone-related processes.

In the second set of experiments (NOACC1, NOACC2, NOACC2.5 and NOACC3 in table 1), the orography is included so that rainfall can form via orographic processes. However, accretion and riming processes are switched off where orographically formed cloud is most likely to be situated (shown by the gray box in Figure 1b). This will limit the production of rainfall via the seeder-feeder mechanism. In the NOACC experiments accretion and riming are switched off below 1 km (NOACC1), 2 km (NOACC2), 2.5 km (NOACC2.5) and 3 km (NOACC3) respectively. Therefore, in these experiments, rainfall produced by orographic processes excluding the seeder-feeder mechanism are present as well as cyclone precipitation. This is shown in Figure 1b and is described by equation

$$E^{NOACC} = a_c + a_{oop}, \tag{2}$$

where E^{NOACC} denotes the accumulated rainfall produced by this experiment and a_{oop} denotes the accumulated rainfall formed via other orographic processes, that is, excluding the low-level accretion and riming associated with the seeder-feeder mechanism.

The final experiment (CTRL experiment in table 1), is a control experiment in which all synoptic scale, mesoscale and microscale mechanisms are included within the model domain. In this experiment, precipitation formed via all mechanisms is produced (shown in Figure 1c). This situation is described by

$$E^{CTRL} = a_c + a_{ar} + a_{oop}, \tag{3}$$

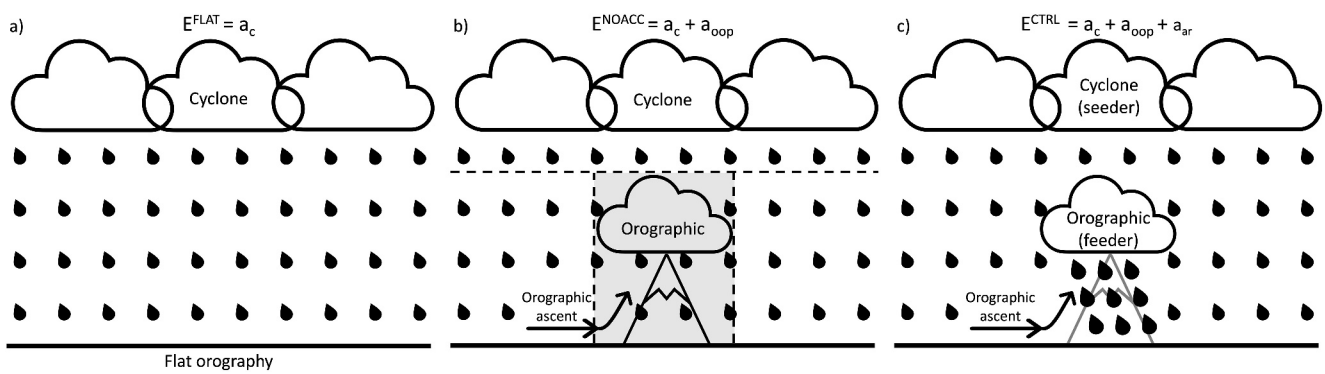

Figure 1. Schematic illustrating experiments conducted using the UKA4g model. (a) represents the FLAT experiment (E^{FLAT}) where the orography is flattened and only cyclone related precipitation is produced (a_c), (b) represents the NOACC experiments (E^{NOACC}) where the gray shaded area represents the region where accretion and riming are not present. Therefore only cyclone related precipitation and other orographic precipitation, excluding the seeder-feeder mechanism are produced (a_c and a_{oop}). The horizontal dashed line represents the altitude (height above mean sea level), and the vertical dashed lines represent the horizontal extent of where accretion and riming are switched off. (c) represents the CTRL experiment (E^{CTRL}) where all mechanisms, including the seeder-feeder mechanism, produce precipitation (a_c, a_{oop} and a_{ar}). The rainfall formed via the seeder-feeder mechanism (a_{ar}) are shown by the large raindrops.

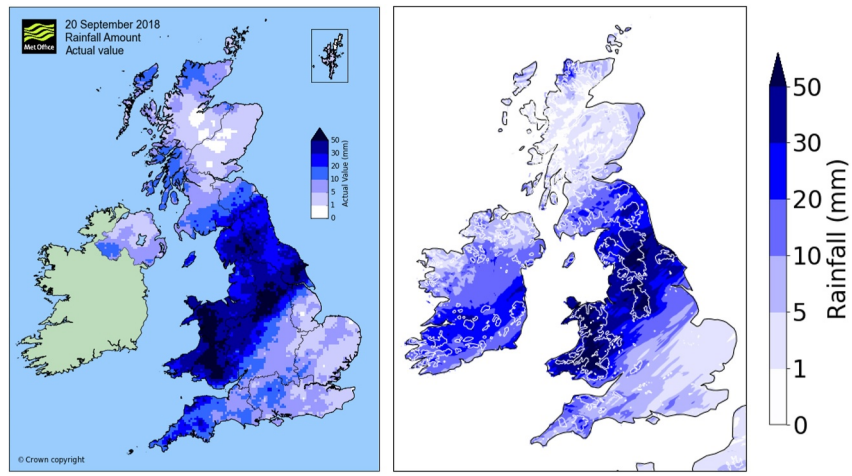

Figure 2. (Left) Had-UK grid 24-hr accumulated rainfall and (right) UKA4g 24-hr accumulated rainfall from 09 UTC 20 September 2018 to 09 UTC 21 September 2018. The white contour represents a 200 m surface height (above mean sea level).

where E^{CTRL} denotes the accumulated rainfall produced by this experiment and a_{ar} denotes the accumulated rainfall formed via low-level accretion and riming.

By switching off the accretion and riming schemes over high orography at different heights, low-level moisture that would have contributed to the production of rainfall is not swept out of the feeder cloud. Therefore, the effects of low-level moisture on the production of rainfall can be investigated. An alternative method to investigate the effects of low level moisture would be to alter the moisture available for the production of precipitation at lower levels. However, this would have other effects, such as modifying rain evaporation. This in turn would have implications for the thermodynamics within the model and the large scale evolution of the simulation. By switching off the accretion and riming schemes over orography rather than over the whole domain, the large scale effects of removing low level moisture can be mitigated.

3. Storm Bronagh

Storm Bronagh originated south of Newfoundland on the 19 September 2018 and intensified from 1,002 hPa on 06 UTC 20 September to 968 hPa 12 UTC on 21 September as it tracked eastwards from the North Atlantic over the UK and into the North Sea. During this time, daily rainfall totals exceeding 50 mm were recorded in upland areas of Wales, the southern Pennines and North York Moors (Met Office, 2018) which lead to localized flooding.

The 24 hr accumulated rainfall in the UK associated with storm Bronagh is shown in Figure 2. To ensure that the UKA4g model aptly captures the accumulated precipitation produced during the passage of storm Bronagh, the 24 hr accumulated rainfall assessed by the Had-UK grid (data interpolated from in-situ observations onto a regular grid (Hollis et al., 2019), Figure 2, left) and the UKA4g model (Figure 2, right) are compared.

It is found that the UKA4g correctly captures the amount and location of the rainfall produced over Wales and the Midlands. This is consistent with S. A. Smith et al. (2015) who demonstrated that on average, orographic precipitation over the UK (including Wales) is accurately reproduced in the MetUM at 1.5 km resolution. Heavy rainfall was located in regions of elevated topography (height above the surface greater than 200 m), suggesting that orographic processes contributed to the formation of this precipitation.

Storm Bronagh developed along a pre-existing atmospheric river over the North Atlantic (Figure 3a). During this time, there was some rainfall associated with the frontal wave that Bronagh develops from, also coinciding with an atmospheric river assessed using integrated vapor transport. The heaviest rainfall lies close to the cyclone center. As the storm continues to develop and track eastwards over the UK (Figure 3b), the heaviest rainfall and atmospheric river centroid (dark green shading) remain close to the cyclone center, bringing rainfall to Ireland, Wales and the UK Midlands. The cold front begins to move eastwards relative to the cyclone center and begins to narrow the warm sector. This continues as the storm moves further inland (Figure 3c). Precipitation forms along both the cold and warm fronts. As the cold front continues to moves eastwards relative to the cyclone center, there

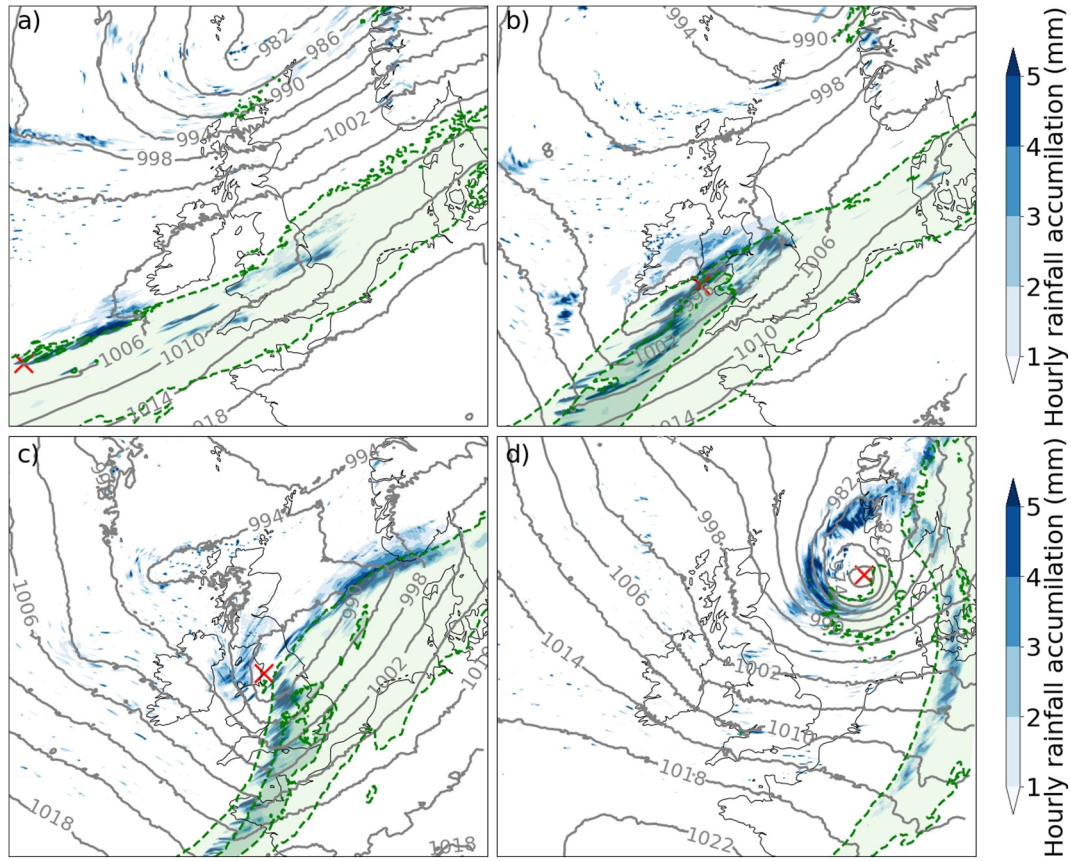

Figure 3. Mean sea level pressure and integrated vapor transport (500 and 1,000 kg m^{-1} s^{-1}, green dashed contours and green shading) at (a) 06 UTC 20 September 2018, (b) 15 UTC 20 September 2018, (c) 00 UTC 21 September 2018 and (d) 12 UTC 21 September 2018, and the hourly accumulated rainfall between (a) 05–06 UTC 20 September 2018, (b) 14–15 UTC 20 September 2018, (c) 23 UTC 20 September 2018 - 00 UTC 21 September 2018 and (d) 11–12 UTC 21 September 2018 produced by the CTRL experiment. The red cross marks the center of the storm at each time-step.

is moisture flux convergence ahead of the front, narrowing the centroid of the atmospheric river, which lies south of the cyclone center ahead of the cold front. As the storm passes over the UK into the North Sea, it continues to intensify, resulting in a comma shaped rainfall pattern. This is consistent with the comma shaped cloud head associated with extratropical cyclones. The atmospheric river continues to move with the cold front as the storm develops further.

4. Results and Discussion

4.1. Vertical Structure of Clouds Over Orography

To ascertain where the orographic and cyclone cloud is situated and therefore, what altitude to switch off accretion and riming, a vertical cross section of the mean cloud liquid water and cloud ice produced over Wales (over a 48 hr period from 00 UTC 20 September 2018 to 00 UTC 22 September 2018) is taken. Hereafter, any value taken over a 48 hr period refers to a period from 00 UTC 20 September 2018 to 00 UTC 22 September 2018. A cross section is taken over Wales as there is rainfall produced by orographic processes (a_{op}) in this location (Figure 4a). The 48 hr accumulated rainfall produced by orographic processes is found by subtracting the 48 hr accumulated rainfall produced by the FLAT experiment from the 48 hr accumulated rainfall produced by the CTRL experiment:

$$a_{op} = a_{oop} + a_{ar} = E^{CTRL} - E^{FLAT}. \quad (4)$$

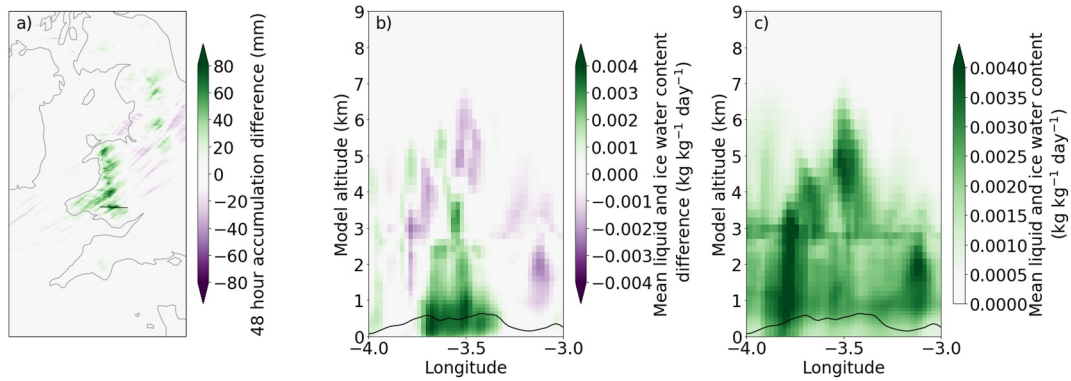

Figure 4. (a) The accumulated rainfall over a 48 hr period due to orographic processes (a_{op}) shown over Wales and England. This is found by subtracting E^{FLAT} from E^{CTRL}. Vertical distribution of mean cloud ice, liquid water content, precipitation and snow over a 48 hr period (b) due to orographic enhancement and (c) produced by the cyclone. The placement of this vertical cross section is represented in (a) by the black line at a latitude of 52.4°N. The *y*-axis in (b) and (c) represents the altitude above the surface (ground level). The height of the surface above mean sea level (orography) is shown by the black line in (b) and (c).

Positive values in Figure 4a represent the rainfall enhancement produced by orographic processes and negative values represent orographic precipitation suppression. Physically, negative values likely represent areas where there is a rain shadow (a region downstream, or on the lee-side of orography, where there is suppressed rainfall) due to the presence of orography.

To ascertain the height below which most orographic cloud water forms, the mean cloud liquid water and cloud ice produced by the FLAT experiment is subtracted from that produced by the CTRL experiment (Figure 4b). Positive values represent the cloud (cloud liquid water and cloud ice content) and snow enhancement due to the presence of orography. Negative values represent a reduction in cloud liquid water, cloud ice and snow amount. Snow is included in this cross-section due to the output of the unified model grouping ice and snow together into a single diagnostic. Negative values downstream (on the lee-side) of orography are likely to be related to the rain shadow where moisture is removed via precipitation over the orography leaving an area of reduced cloud on the lee-side. Negative values above 3 km are more difficult to interpret but may be related to orographic processes occurring upstream.

The majority of the orographic-related cloud enhancement is located below 3 km above ground level. The mean cloud liquid water and cloud ice produced by the cyclone in the FLAT experiment is shown in Figure 4c. The cyclone-related cloud extends from 0 to 7 km above mean sea level (Figure 4c). Since the majority of the orographic-related cloud is located below 3 km, the accretion and riming schemes are switched off below 1, 2, 2.5 and 3 km. Since orographic rainfall is produced where the orography is greater than 200 m, the schemes are switched off in these regions only. This ensures the synoptic scale dynamics of storm Bronagh are not altered significantly in the model domain (not shown).

4.2. Precipitation Mechanisms

Equation 1 gives the contribution from cyclone related precipitation which comes from the FLAT experiment as no orography (and therefore no orographic precipitation) is present. The contribution from the other orographic processes (excluding the seeder-feeder mechanism) is found by subtracting the accumulated rainfall in the FLAT experiment from the NOACC experiments:

$$a_{oop} = E^{NOACC} - E^{FLAT}. \quad (5)$$

The contribution from low-level accretion and riming (i.e., the seeder-feeder mechanism) is found by subtracting the accumulated rainfall from the NOACC experiments from the CTRL experiment:

$$a_{ar} = E^{CTRL} - E^{NOACC}. \quad (6)$$

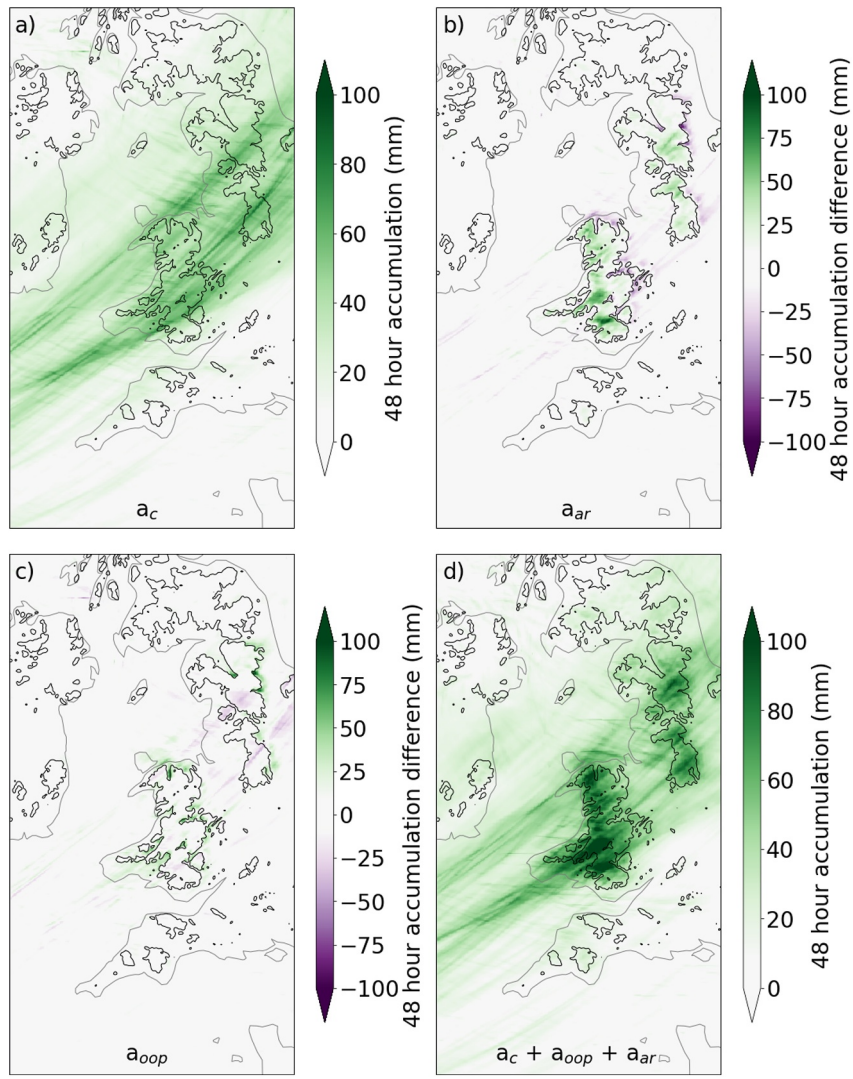

Figure 5. 48 hour rainfall accumulation (mm) produced by (a) cyclone related processes, a_c, (b) accretion and riming, a_{ar}, (c) other orographic processes, a_{oop}, (d), all processes.

To understand how much each mechanism contributes to the rainfall produced during the passage of storm Bronagh over the UK, maps of the 48 hr accumulated rainfall over the UK (with focus on Wales where the topography is greater than 200 m above mean sea level) are created. We focus on Wales as this is on the west coast of the UK, meaning that the storm will not have encountered any orography yet as it tracked westwards over the Atlantic (Figure 3).

The 48 hr accumulated rainfall formed via each mechanism is shown in Figure 5. The accumulated rainfall produced by the cyclone, a_c, is shown in Figure 5a where the accumulated rainfall extends from the SW to the NE as the cyclone tracks over the UK. Figure 5b shows the rainfall accumulation due to orographic accretion and riming processes, a_{ar}. The seeder-feeder mechanism enhances rainfall over the hills in Wales by up to 50 mm. A small region of negative values can been seen eastwards of the 200 m contour. When the accretion and riming schemes are switched off, there is more moisture available to produce rainfall downstream of the orography which otherwise would have been converted to precipitation via accretion and riming. This moisture is not present in the CTRL experiment as the accretion and riming schemes are not modified. Therefore, there is a rain shadow on the leeward side of the hills. Figure 5c shows the rainfall accumulation due to other orographic processes, a_{oop}. This term is small compared to the cyclone and seeder-feeder processes and suggests that forced ascent over hills and orographically forced convection do not influence precipitation rates significantly in this case.

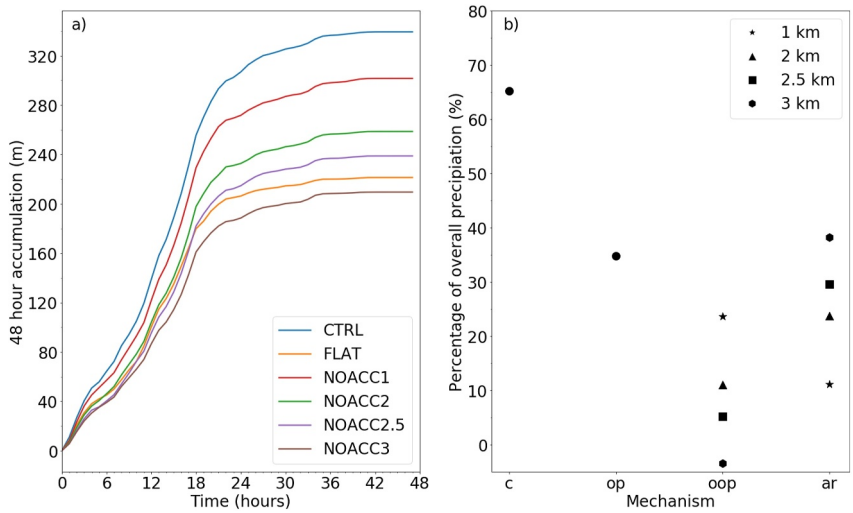

Figure 6. (a) Rainfall accumulation (mm) over a 48 hr period. Experiments described in Table 1, CONTROL (blue), FLAT (yellow), NOACC1 (red), NOACC2 (green), NOACC2.5 (purple) and NOACC3 (brown). (b) Contribution of different mechanisms to 48 hr accumulated precipitation total. Cyclone-related processes (a_c), orographic processes (a_op), other orographic processes (a_{oop}) and accretion and riming (a_{ar}). Simulations in which accretion and riming is switched off below 1 km (star), 2 km (triangle), 2.5 km (square) and 3 km (circle).

To quantify how much each mechanism contributes to the rainfall produced, the accumulated rainfall produced by each experiment is calculated over a 48 hr period in hourly increments where the surface height is greater than 200 m in Wales. At each time-step a rectangular region (63 × 108 km) of the hourly accumulated rainfall over Wales (centered at (52.4°N, 3.7°W)) is taken. Subsequently, the integral over a surface elevation greater than 200 m within this rectangle is calculated.

The accumulated rainfall produced by each experiment over a 48 hr period is shown in Figure 6a. The accumulated rainfall produced by each experiment rapidly increases from 0 to 18 hr in each experiment as the storm tracks over Wales (Figures 3a and 3b). The accumulated rainfall then increases at a slower rate which coincides with the storm moving across the UK into the North Sea (Figure 3c). Finally, at approximately 36 hr the accumulated rainfall plateaus as the storm passes into Scandinavia (Figure 3d). The CTRL experiment produces the most rainfall as all processes are present in this experiment. The NOACC experiments produce less accumulated rainfall the higher the altitude that the accretion and riming schemes are switched off at. This is because the higher the altitude, the more the droplet growth is limited in the cloud. As there is only cyclone related precipitation present in the FLAT experiment, this experiment is expected to produce the least amount of rainfall. However, there is less rainfall produced in the NOACC3 experiment than the FLAT experiment. This suggests that in NOACC3 switching off accretion and riming is restricting precipitation formation within the cyclone-produced cloud at altitudes greater than 2.5 km.

The percentage of the 48 hr accumulated rainfall that is produced by each mechanism is shown in Figure 6b. It is found that 63% of the rainfall associated with storm Bronagh was produced by cyclone-related processes (frontal ascent and embedded convection) and 37% produced via orographic processes. Therefore, the majority of the rainfall associated with the storm is produced by the cyclone. Through the modification of the accretion and riming schemes at different heights the contribution from the seeder-feeder mechanism and other orographic processes (forced ascent, forced convection) can be determined. It is found that the seeder-feeder mechanism, a_{ar}, contributes a larger amount (30%) to precipitation than other orographic processes (7%), when accretion and riming at heights up to 2.5 km above ground level is attributed to the seeder-feeder mechanism. When accretion and riming up to 3 km above ground level is attributed to the seeder-feeder mechanism, the percentage of rainfall produced by this mechanism exceeds the total for all orographic processes suggesting that accretion and riming in the cyclone cloud between 2.5 and 3 km is been incorrectly attributed to the seeder-feeder mechanism. When accretion and riming below 1 km only is attributed to the seeder-feeder mechanism, other orographic processes contribute more to precipitation totals than the seeder-

feeder mechanism. However, the precipitation due to other orographic processes occurs around the edges of the hill not over the hill (Figure 5c). Since the orographically enhanced liquid and ice water content extends from the ground to above 2 km this suggests that the seeder-feeder mechanism occurring through the whole depth of the orographic cloud (0–2.5 km above ground level) is important for enhancing precipitation, not just the lowest 1 km. Higher levels may also be important, but it is difficult to isolate orographic enhancement at higher levels due to the presence of cyclone related water.

5. Conclusions

Through the investigation of the precipitation produced by storm Bronagh and the associated atmospheric river as it passed over the UK, it is found that 63% of the rainfall over the hills in Wales is produced by cyclone-related processes (frontal ascent and convection). The other 37% is produced via orographic processes, mainly the seeder-feeder mechanism. Thus the cyclone precipitation is increased by 50% by the presence of orography. The orography redistributes where surface rain occurs, focusing more of the rain over the hills, which may run into valleys, producing flooding. Simulating these processes at high resolution (1.5 km) allows us to capture these effects. Lower-resolution simulations do not accurately represent the important scales of orography, particularly the small-scales hills of the UK and so need seeder-feeder parameterization schemes to correct for this defect (S. A. Smith et al., 2016; S. A. Smith et al., 2019).

Studies such as Hill et al. (1981); B. Smith et al. (2010); Neiman et al. (2011) and Lean and Browning (2013) show that the amount of enhancement via the seeder-feeder mechanism is linked to the availability of low-level moisture and the strength of the low-level winds. This is supported by this study through switching off accretion and riming at different heights over regions of high orography. It is demonstrated that in storm Bronagh, the forced ascent of moist air within the atmospheric river over the hills increases the water content in the lowest 2.5 km above the ground. Accretion and riming processes in the lowest 2.5 km allow the cyclone-related precipitation to grow rapidly, enhancing precipitation rates over orography.

Other authors have indirectly inferred the importance of the seeder-feeder mechanism to the enhancement of precipitation (e.g., (Bader & Roach, 1977; Browning et al., 1974; Browning & Mason, 1980; Lean & Browning, 2013; Rössler et al., 2014; Thomas et al., 2023)). The results presented in this study support the previous findings that infer the importance of the seeder-feeder mechanism to the enhancement of precipitation. However, this study quantifies and compares how much rainfall is produced by the cyclone and by the enhancement of precipitation. We demonstrate that cyclone-related precipitation dominates precipitation totals, but that the seeder-feeder mechanism leads to significant enhancement of pre-existing cyclone related rainfall. To the authors knowledge, this is the first time the enhancement of rainfall via the seeder-feeder mechanism has been switched off in simulations and hence directly quantified.

This study has introduced a novel methodology that quantifies the amount of precipitation produced via different mechanisms. This methodolology can be applied to case studies in other geographic locations where the orography might be much higher and wider than it is in the UK. This would give further insight into the importance of each mechanism in the formation of precipitation when an atmospheric river and extratropical cyclone make landfall. It is useful to note that in case studies where the mountains are higher, the effect of the height of the freezing level would need to be taken into consideration as the freezing level could be a similar height to the orography. This can affect the amount of frozen precipitation produced. If less frozen precipitation is produced, the risk increases for associated natural hazards such as landslides and floods (Nash et al., 2024).

Another limitation of this study is that only one numerical model is used to simulate the case study. Previous studies have shown that atmospheric river related precipitation is sensitive to the microphysics parameterisation and boundary layer parameterisation used (Toride et al., 2019). Therefore, further work could involve reproducing these results with a variety of models.

Despite these limitations, this study provides a methodology for use in future studies that aim to quantify the contributions of different mechanisms to the formation of precipitation in different geographic locations. This is especially prevalent for the case of land-falling atmospheric rivers as their intensity is expected to increase as the climate warms and there is an increase in atmospheric moisture (Allan et al., 2020).

Data Availability Statement

HadUK-Grid v1.0.0.0 is available through the Centre for Environmental Data Analysis (CEDA). The model simulations were produced with the Met Office Unified Model (UM) run using Rose and Cylc. The source code for the UM is free to use. However, software for this research is not publicly available due to licensing restrictions. The Rose and Cylc software used to drive the Unified Model are public at (Met Office, 2008; Met Office, 2012) respectively.

Acknowledgments
S. Cuckow was supported by National Environmental Research Council (NERC) Doctoral Training Grant (Grant F4114905). O Martínez-Alvarado was supported by NERC through the UK National Centre for Atmospheric Science (NCAS) (Grant R8/H12/83/007).

References

Allan, R. P., Barlow, M., Byrne, M. P., Cherchi, A., Douville, H., Fowler, H. J., et al. (2020). Advances in understanding large-scale responses of the water cycle to climate change. *Annals of the New York Academy of Sciences*, *1472*(1), 49–75. https://doi.org/10.1111/nyas.14337

Allan, R. P., Lavers, D. A., & Champion, A. J. (2016). Diagnosing links between atmospheric moisture and extreme daily precipitation over the UK. *International Journal of Climatology*, *36*(9), 3191–3206. https://doi.org/10.1002/joc.4547

AMS. (2023). *Rain shadow American meteorology society*. Glossary of Meteorology

Bader, M. J., & Roach, W. T. (1977). Orographic rainfall in warm sectors of depressions. *Quarterly Journal of the Royal Meteorological Society*, *103*(436), 269–280. https://doi.org/10.1256/smsqj.43604

Browning, K. A. (1971). Radar measurements of air motion near fronts. *Weather*, *26*(8), 320–340. https://doi.org/10.1002/j.1477-8696.1971.tb07416.x

Browning, K. A., Hill, F. F., & Pardoe, C. W. (1974). Structure and mechanism of precipitation and the effect of orography in a wintertime warm sector. *Quarterly Journal of the Royal Meteorological Society*, *100*(425), 309–330. https://doi.org/10.1002/qj.49710042505

Browning, K. A., & Mason, J. S. (1980). Air motion and precipitation growth in frontal systems. *Pure and Applied Geophysics*, *119*(3), 577–593. https://doi.org/10.1007/978-3-0348-5148-0_11

Carlson, T. N. (1980). Airflow through midlatitude cyclones and the comma cloud pattern. *Monthly Weather Review*, *108*(10), 1498–1509. https://doi.org/10.1175/1520-0493(1980)108⟨1498:ATMCAT⟩2.0.CO;2

Champion, A. J., Allan, R. P., & Lavers, D. A. (2015). Atmospheric rivers do not explain UK summer extreme rainfall. *Journal of Geophysical Research: Atmospheres*, *120*(14), 6731–6741. https://doi.org/10.1002/2014JD022863

Cuckow, S., Dacre, H. F., & Martínez-Alvarado, O. (2022). Moisture transport contributing to precipitation at the centre of storm Bronagh. *Weather*, *77*(6), 196–201. https://doi.org/10.1002/wea.4212

Dacre, H. F., Clark, P. A., Martinez-Alvarado, O., Stringer, M. A., & Lavers, D. A. (2015). 09). How do atmospheric rivers form? *Bulletin of the American Meteorological Society*, *96*(8), 1243–1255. https://doi.org/10.1175/BAMS-D-14-00031.1

Dacre, H. F., Martínez-Alvarado, O., & Mbengue, C. O. (2019). 06). Linking atmospheric rivers and warm conveyor belt airflows. *Journal of Hydrometeorology*, *20*(6), 1183–1196. https://doi.org/10.1175/JHM-D-18-0175.1

Davies, T. (2014). Lateral boundary conditions for limited area models. *Quarterly Journal of the Royal Meteorological Society*, *140*(678), 185–196. https://doi.org/10.1002/qj.2127

Gentile, E., Barlow, J., Edwards, J., Lewis, H., & Gray, S. (2021). The impact of atmosphere-ocean-wave coupling on the near-surface wind speed in forecasts of extratropical cyclones. *Boundary-Layer Meteorology*, *180*(1), 105–129. https://doi.org/10.1007/s10546-021-00614-4

Gimeno-Sotelo, L., & Gimeno, L. (2023). Where does the link between atmospheric moisture transport and extreme precipitation matter? *Weather and Climate Extremes*, *39*, 100536. https://doi.org/10.1016/j.wace.2022.100536

Hawcroft, M. K., Shaffrey, L. C., Hodges, K. I., & Dacre, H. F. (2012). How much Northern Hemisphere precipitation is associated with extratropical cyclones? *Geophysical Research Letters*, *39*(24). https://doi.org/10.1029/2012GL053866

Hill, F. F., Browning, K. A., & Bader, M. J. (1981). Radar and raingauge observations of orographic rain over south wales. *Quarterly Journal of the Royal Meteorological Society*, *107*(453), 643–670. https://doi.org/10.1002/qj.49710745312

Hollis, D., McCarthy, M., Kendon, M., Legg, T., & Simpson, I. (2019). Haduk-grid—A new UK dataset of gridded climate observations. *Geoscience Data Journal*, *6*(2), 151–159. https://doi.org/10.1002/gdj3.78

Kingston, D. G., Lavers, D. A., & Hannah, D. M. (2016). Floods in the southern alps of New Zealand: The importance of atmospheric rivers. *Hydrological Processes*, *30*(26), 5063–5070. https://doi.org/10.1002/hyp.10982

Kropač, E., Mölg, T., Cullen, N. J., Collier, E., Pickler, C., & Turton, J. V. (2021). A detailed, multi-scale assessment of an Atmospheric River event and its impact on extreme glacier melt in the southern alps of New Zealand. *Journal of Geophysical Research: Atmospheres*, *126*(9). https://doi.org/10.1029/2020JD034217

Lamjiri, M. A., Dettinger, M. D., Ralph, F. M., & Guan, B. (2017). Hourly storm characteristics along the U.S. West Coast: Role of atmospheric rivers in extreme precipitation. *Geophysical Research Letters*, *44*(13), 7020–7028. https://doi.org/10.1002/2017GL074193

Lavers, D. A., Allan, R. P., Villarini, G., Lloyd-Hughes, B., Brayshaw, D. J., & Wade, A. J. (2013). Future changes in atmospheric rivers and their implications for winter flooding in britain. *Environmental Research Letters*, *8*(3), 034010. https://doi.org/10.1088/1748-9326/8/3/034010

Lavers, D. A., Allan, R. P., Wood, E. F., Villarini, G., Brayshaw, D. J., & Wade, A. J. (2011). Winter floods in Britain are connected to atmospheric rivers. *Geophysical Research Letters*, *38*(23), 1–8. https://doi.org/10.1029/2011GL049783

Lean, H. W., & Browning, K. A. (2013). Quantification of the importance of wind drift to the surface distribution of orographic rain on the occasion of the extreme Cockermouth flood in Cumbria. *Quarterly Journal of the Royal Meteorological Society*, *139*(674), 1342–1353. https://doi.org/10.1002/qj.2024

Lewis, H., Sanchez, J., Arnold, A., Fallmann, J., Saulter, A., Graham, J., et al. (2019). The UKC3 regional coupled environmental prediction system. *Geoscientific Model Development*, *12*(6), 2357–2400. https://doi.org/10.5194/gmd-12-2357-2019

Little, K., Kingston, D. G., Cullen, N. J., & Gibson, P. B. (2019). The role of atmospheric rivers for extreme ablation and snowfall events in the southern alps of New Zealand. *Geophysical Research Letters*, *46*(5), 2761–2771. https://doi.org/10.1029/2018GL081669

Met Office. (2008). Cycl software and documentation [software]. Retrieved from https://cylc.github.io/ (Accessed on 4 July 2024)

Met Office. (2012). Rose software and documentation [software]. Retrieved from https://github.com/metomi/rose (Accessed on 4 July 2024)

Met Office. (2018). Strong winds and heavy rain from storms ali and bronagh. Retrieved from https://www.metoffice.gov.uk/binaries/content/assets/metofficegovuk/pdf/weather/learn-about/uk-past-events/interesting/2018/strong-winds-and-heavy-rain-from-storms-ali-and-bronagh---met-office.pdf ([Accessed 25 November 2021])

Michel, C., Sorteberg, A., Eckhardt, S., Weijenborg, C., Stohl, A., & Cassiani, M. (2021). Characterization of the atmospheric environment during extreme precipitation events associated with atmospheric rivers in Norway - seasonal and regional aspects. *Weather and Climate Extremes*, *34*, 100370. https://doi.org/10.1016/j.wace.2021.100370

Nash, D., Carvalho, L. M. V., Rutz, J. J., & Jones, C. (2024). Influence of the freezing level on atmospheric rivers in high mountain asia: Wrf case studies of orographic precipitation extremes. *Climate Dynamics*, *62*(1), 589–607. https://doi.org/10.1007/s00382-023-06929-x

Neiman, P., Schick, L., Ralph, F., Hughes, M., & Wick, G. (2011). Flooding in western Washington: The connection to atmospheric rivers. *Journal of Hydrometeorology*, *12*(6), 1337–1358. https://doi.org/10.1175/2011jhm1358.1

Oertel, A., Sprenger, M., Joos, H., Boettcher, M., Konow, H., Hagen, M., & Wernli, H. (2021). Observations and simulation of intense convection embedded in a warm conveyor belt–how ambient vertical wind shear determines the dynamical impact. *Weather and Climate Dynamics*, *2*(1), 89–110. https://doi.org/10.5194/wcd-2-89-2021

Oltmanns, M., Straneo, F., & Tedesco, M. (2018). Increased Greenland melt triggered by large-scale, year-round precipitation events. *The Cryosphere Discuss*.

Pfahl, S., Madonna, E., Boettcher, M., Joos, H., & Wernli, H. (2014). Warm conveyor belts in the ERA-interim dataset (1979–2010). Part II: Moisture origin and relevance for precipitation. *Journal of Climate*, *27*(1), 27–40. https://doi.org/10.1175/JCLI-D-13-00223.1

Pfahl, S., & Wernli, H. (2012). Quantifying the relevance of cyclones for precipitation extremes. *Journal of Climate*, *25*(19), 6770–6780. https://doi.org/10.1175/JCLI-D-11-00705.1

Ralph, F. M., Neiman, P. J., & Wick, G. A. (2004). Satellite and CALJET aircraft observations of atmospheric rivers over the eastern north Pacific ocean during the winter of 1997/98. *Monthly Weather Review*, *132*(7), 1721–1745. https://doi.org/10.1175/1520-0493(2004)132⟨1721:SACAOO⟩2.0.CO;2

Ralph, F. M., Neiman, P. J., Wick, G. A., Gutman, S. I., Dettinger, M. D., Cayan, D. R., & White, A. B. (2006). Flooding on California's Russian River: Role of atmospheric rivers. *Geophysical Research Letters*, *33*(13), 3–7. https://doi.org/10.1029/2006GL026689

Ramos, A. M., Trigo, R. M., Liberato, M. L. R., & Tomé, R. (2015). Daily precipitation extreme events in the Iberian Peninsula and its association with atmospheric rivers. *Journal of Hydrometeorology*, *16*(2), 579–597. https://doi.org/10.1175/JHM-D-14-0103.1

Reid, K. J., Rosier, S. M., Harrington, L. J., King, A. D., & Lane, T. P. (2021). Extreme rainfall in New Zealand and its association with atmospheric rivers. *Environmental Research Letters*, *16*(4), 44012. https://doi.org/10.1088/1748-9326/abeae0

Roe, G. H. (2005). Orographic precipitation. *Annual Review of Earth and Planetary Sciences*, *33*(1), 645–671. https://doi.org/10.1146/annurev.earth.33.092203.122541

Rössler, O., Froidevaux, P., Börst, U., Rickli, R., Martius, O., & Weingartner, R. (2014). Retrospective analysis of a nonforecasted rain-on-snow flood in the alps Äì a matter of model limitations or unpredictable nature? *Hydrology and Earth System Sciences*, *18*(6), 2265–2285. https://doi.org/10.5194/hess-18-2265-2014

Rutz, J. J., James Steenburgh, W., & Martin Ralph, F. (2014). Climatological characteristics of atmospheric rivers and their inland penetration over the western United States. *Monthly Weather Review*, *142*(2), 905–921. https://doi.org/10.1175/MWR-D-13-00168.1

Smith, B., Yuter, S., Neiman, P., & Kingsmill, D. (2010). 01). Water vapor fluxes and orographic precipitation over northern California associated with a landfalling atmospheric river. *Monthly Weather Review*, *138*(1), 74–100. https://doi.org/10.1175/2009MWR2939.1

Smith, S. A., Field, P. R., Vosper, S. B., & Derbyshire, S. H. (2019). Verification of a seeder–feeder orographic precipitation enhancement scheme accounting for low-level blocking. *Quarterly Journal of the Royal Meteorological Society*, *145*(724), 2909–2932. https://doi.org/10.1002/qj.3584

Smith, S. A., Field, P. R., Vosper, S. B., Shipway, B. J., & Hill, A. A. (2016). A parametrization of subgrid orographic rain enhancement via the seeder–feeder effect. *Quarterly Journal of the Royal Meteorological Society*, *142*(694), 132–142. https://doi.org/10.1002/qj.2637

Smith, S. A., Vosper, S. B., & Field, P. R. (2015). Sensitivity of orographic precipitation enhancement to horizontal resolution in the operational Met Office Weather forecasts. *Meteorological Applications*, *22*(1), 14–24. https://doi.org/10.1002/met.1352

Thomas, J., Barrett, A., & Hoose, C. (2023). Temperature and cloud condensation nuclei (ccn) sensitivity of orographic precipitation enhanced by a mixed-phase seeder–feeder mechanism: A case study for the 2015 cumbria flood. *Atmospheric Chemistry and Physics*, *23*(3), 1987–2002. https://doi.org/10.5194/acp-23-1987-2023

Toride, K., Iseri, Y., Duren, A. M., England, J. F., & Kavvas, M. L. (2019). Evaluation of physical parameterizations for atmospheric river induced precipitation and application to long-term reconstruction based on three reanalysis datasets in western Oregon. *Science of the Total Environment*, *658*, 570–581. https://doi.org/10.1016/j.scitotenv.2018.12.214

Valiente, N. G., Saulter, A., Edwards, J. M., Lewis, H. W., Castillo Sanchez, J. M., Bruciaferri, D., et al. (2021). The impact of wave model source terms and coupling strategies to rapidly developing waves across the North-west European shelf during extreme events. *Journal of Marine Science and Engineering*, *9*(4), 403. https://doi.org/10.3390/jmse9040403

Xu, G., Wang, L., Chang, P., Ma, X., & Wang, S. (2022). Improving the understanding of atmospheric river water vapor transport using a three-dimensional straightened composite analysis. *Journal of Geophysical Research: Atmospheres*, *127*(11), e2021JD036159. (e2021JD036159 2021JD036159. https://doi.org/10.1029/2021JD036159